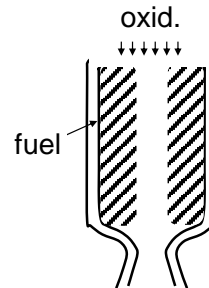


Hybrid Rockets

Background

- Combination of liquid and solid rockets
 - one propellant “solid” (usually fuel)
 - 2nd propellant liquid or gas (oxid.)
- Early history
 - 1930’s combustion tests of
 - coal and $N_2O(g)$ at I.G. Farben, Germany
 - coal and GOX by Calif. Rocket Soc.
 - tar-wood-saltpeter and LOX by Hermann Oberth (von Braun’s teacher), Germany
 - 1933 flight test GIRD-09 (15 s duration, 400m alt., 1.5 km distance)
 - gasoline-gum gel (“solid”) on metal frame and pressurized LOX, Mikhail Tikhonravov and Sergei Korolev www.russianspaceweb.com/gird09.html credit: ARRAN



Hybrid Rockets: 1950-1970's

- Mostly tests of polymer fuels and numerous oxidizers
 - GE: 1951-1956 (Moore), polyethylene and 90% H_2O_2
 - demonstrated throttling by valve but low burning rates
 - APL (JHU), Thiokol, UTC: 1950's tested inverse hybrids (liquid fuel, solid ox)
 - poor success
 - UTC/NASA: mid 1960's-1970 hypergolic hybrid, PBAN impregnated with Li, LiH; and FLOx (30% F_2 , 70% O_2)
 - 380 s Isp
 - Volvo/Svenska Flygmotor: 1965-1971
 - 1965 HR-3F, PB with aromatic amine (Tagaform) fuel and white fuming nitric acid (WFNA) oxidizer
 - flight test reached 4.2 km alt, 6.2 s duration, 30 g max accel.
 - UTC: 1968 Sandpiper target drone, PMMA/Mg fuel and Mon25 (N_2O_4 , NO_2 and 25% NO)
 - 300 s duration, 8:1 throttle ratio, level flight up to 160 km alt



from A. Ingemar Skoog, Swedish Sounding Rocket Projects, IAC-06-E4.4.02

Hybrid Rockets 3
Copyright © 2007, 2017, 2019 by Jerry M. Seltman. All rights reserved.

AE6450 Rocket Propulsion

Hybrid Rockets: 1980's-2000's (US)

- 1983 Teledyne Firebolt: air-launched target drone entered USAF service, CSD-UTC hybrid rocket
 - ram air turbine pressurized IRFNA, PMMA/PB solid fuel
 - 10:1 throttle (120-1200 lbf)
- 1984 Starstruck's Dolphin rocket (James Bennett)
 - HTPB and LOX
 - 175kN thrust, follow-on tests at AMROC: up to 324 kN (H-500)
- 1999-2002 NASA-DARPA initiated program (ground test NASA Stennis)
 - 70" D, 45 ft L, 250klbf (1.1 MN) thrust, T/W=2, 27 s burn duration
- 2004 small hybrid (HTPB- N_2O ; 88kN) used to launch Space Ship one



USAF museum



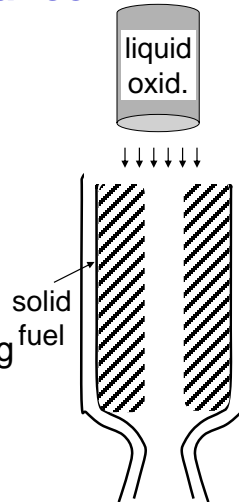
Courtesy of XPRIZE Foundation
Discovery Channel & Virgin Galactic, Inc.

Hybrid Rockets 4
Copyright © 2007, 2017, 2019 by Jerry M. Seltman. All rights reserved.

AE6450 Rocket Propulsion

Hybrid Rocket Performance

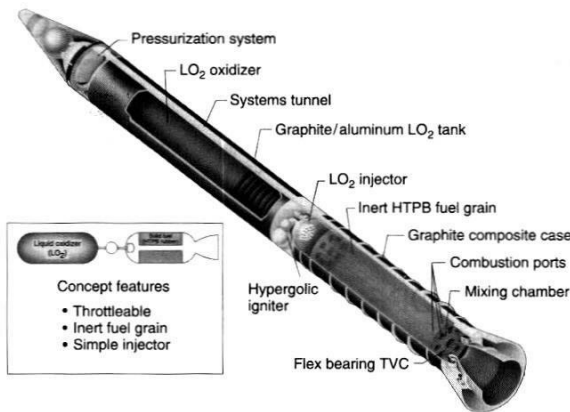
- Compared to SRM's and LRE's
 - intermediate specific impulse, density-specific impulse, complexity
 - control: restart, throttleable
 - improved safety vs. solids (no detonation/explosion)
 - specific impulse O/F varies during burn
 - lower regression rate than solids
 - higher fraction of unburned solid after burn



Hybrid Rockets 5
Copyright © 2007, 2017, 2019 by Jerry M. Seltman. All rights reserved.

AE6450 Rocket Propulsion

Example – SRM Replacement



- Pressurization
 - similar options to liquid rockets: gas, turbopump (expander, tap-off, ...)
- Oxidizer pre-vaporization
- Final volume for propellants to finish burning since not mixed initially
 - combustion efficiency of 90-95% considered pretty good

FIGURE 15-1. Large hybrid rocket booster concept capable of boosting the Space Shuttle. It has an inert solid fuel grain, a pressurized liquid oxygen feed system, and can be throttled. from Sutton

Hybrid Rockets 6
Copyright © 2007, 2017, 2019 by Jerry M. Seltman. All rights reserved.

AE6450 Rocket Propulsion

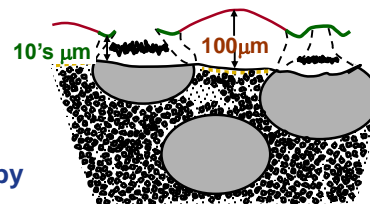
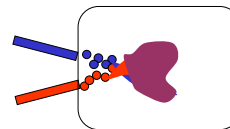
Hybrid Rockets

Regression Rate and Internal Ballistics

Combustion “Rate”

- Major difference from liquid bipropellant and solid technologies is due to combustion process
- Processes limiting burn rate are:
 - mass injection rate
 - mixing (often requires conversion to gas)
 - heat transfer
 - chemistry (generally fast)
- **Liquid bipropellants**, pressurization system controls mass injection, combustion **primarily limited by mixing rate**
- **Solid propellants**, well mixed (at least within 10-100 μm), combustion **limited by mass injection**, depends on **heat transfer** from flame to surface

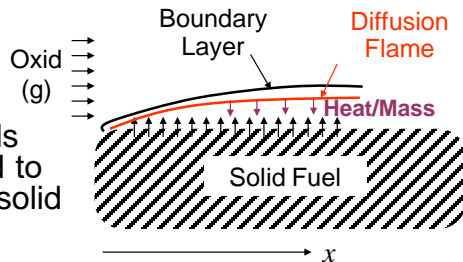
Liquid Bipropellant



Solid (Composite) Propellant

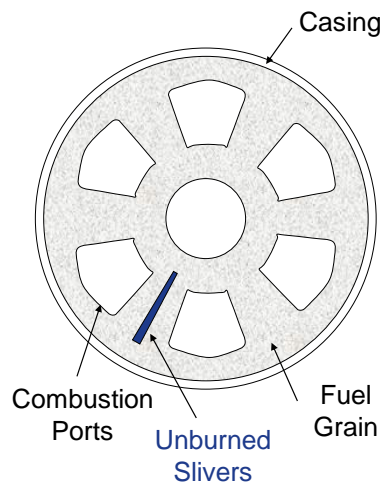
Hybrid Regression Rate

- Hybrid combustion rate
 - limited by conversion of solid fuel to gas
 - gas needs to “diffuse” toward oxidizer across boundary layer
 - heat from flame needs to “diffuse” downward to drive vaporization of solid fuel
- Varies downstream
 - as boundary layer/flame distance changes
 - fuel mass injection varies along port length
- Depends on oxidizer injection rate



Multiport Fuel Grains

- Hybrids generally have lower regression rate than solid propellants
 - higher burn area required to achieve high thrust
 - use multiple ports
 - also reduces distance to oxidizer stream
- More complex casting required
- Unburned “slivers”
 - left over or broken off



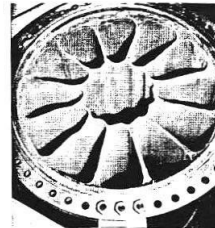
Example - Unburned Fuel

- Remaining unburned fuel
 - wasted mass
 - lower effective density-specific impulse

Before burn



After burn



some solid fuel remaining on struts (structural supports)

From Figure 7.19 Humble

Hybrid Regression Rate

- Hybrid burning rate limited by heat transfer back to solid fuel
 - similar issue seen in **erosive burning** of solid propellants
 - recall Lenoir-Robillard model (1957) based on heat transfer boundary layer

$$r_e \propto \frac{c_p}{c_s} \frac{(\mu/D)^{0.2}}{\rho_s} Pr^{-2/3} \frac{T_o - T_s}{T_s - T_p} G_\infty^{0.8} e^{-const \frac{(\rho u)_{burn}}{G_\infty}}$$

“blowing” ratio of mass fluxes

Analytic Hybrid Regression Rate

- So we expect solid fuel regression rate in hybrid to be function of

$$r_{\text{hybrid}} = f(G_{\infty}, \mu, G_{\text{solid}}/G_{\infty}, x, \dots)$$

- unlike solid propellant, $r \propto p_o^n$
no direct pressure dependence

- From analysis of *convective* heat transfer in turbulent boundary layer over flat plate with blowing,

$$r_{\text{hybrid}} = 0.036 \frac{G_{\infty}^{0.8}}{\rho_{\text{sf}}} \left(\frac{\mu}{x} \right)^{0.2} \beta^{0.23} \quad \text{Eq. 16-1 in Sutton}$$

$$\text{Blowing Coefficient } \beta \equiv \frac{G_{\text{solid}}}{G_{\infty}} St^{-1} Pr^{-2/3} \quad Pr = \frac{\nu}{\alpha}; St = \frac{h}{\rho_{\infty} u_{\infty} c_p}$$

Regression Rate Dependence

$$r_{\text{hybrid}} = 0.036 \frac{G_{\infty}^{0.8}}{\rho_{\text{sf}}} \left(\frac{\mu}{x} \right)^{0.2} \beta^{0.23}$$

- Increases with local free stream mass flux ($G_{\infty} = \text{oxid.} + \text{fuel} + \text{products}$)
 - G_{∞} typically increases downstream
- $1/x$ dependence
 - due to boundary layer growth
- Increases with relative importance of injection from solid
 - can show (see A.5 Sutton 7th ed.) $\beta \sim \frac{T_{\text{flame}} - T_{\text{surface}}}{\Delta h_{\text{vap, surface}}}$ *high $\beta \Rightarrow$ hot flame or easily vaporized solid*
- **Ignores**
 - curvature and **radiative heat transfer** (e.g., metalized solids, which also tend to increase T_{flame})

Empirical Local Regression Rate Models

- Ignoring blowing and for given system

$$r_{\text{hybrid}} = aG_{\infty}^n x^{-m} \quad \text{e.g., O}_2\text{-HTPB, empirical results indicate } n \sim 0.75\text{-}0.77; m \sim 0.14\text{-}0.16$$

close to turb. b.l. model

- Some empirical data suggests

$$r_{\text{hybrid}} = aG_{\text{ox}}^n p_o^k D_p^l$$

– observed pressure and port diameter dependence

- Ballistic performance scaling of hybrids complex, less understood – **harder to design**

Average Burn Rate

- Above are regression rates at some local distance along port (x)
- Useful to have avg. regression rate

$$\dot{m}_{f,\text{total}} = r_{\text{avg}} \rho_s A_b$$

- Def'n.

$$r_{\text{avg}} \equiv \frac{1}{x} \int_0^x r(x') dx'$$

$$D_p = \frac{4A_x}{S}$$

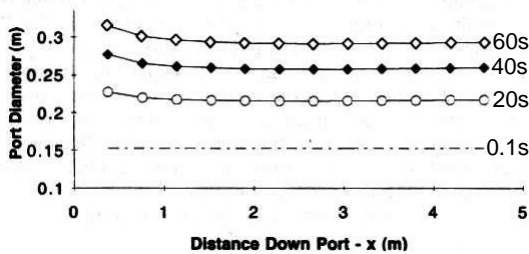

- Examine using

$$r = aG_{\infty}^n x^{-m} = a(G_{\text{ox}} + G_f(x))^n x^{-m} \quad G_f(x) = 4\rho_s \int_0^x \frac{r(x')}{D_p(x')} dx'$$

Average Burn Rate

$$r(x) = a \left[G_{ox} + 4\rho_s \int_0^x \frac{r(x')}{D_P(x')} dx' \right]^n x^{-m}$$

- Can often assume $D_P \neq D_P(x)$



$G_{\infty} \uparrow$ downstream
offset by b.l. growth

From Figure 7.7 Humble
(calculations based on
given propellant data)

$$r(x) = a \left[G_{ox} + 4 \frac{\rho_s}{D_P} \int_0^x \overbrace{r(x') dx'}^{\equiv I_r} \right]^n x^{-m} \quad r(x) = \frac{dI_r}{dx}$$

Hybrid Rockets 17
Copyright © 2007, 2017, 2019 by Jerry M. Seltman. All rights reserved.

AE6450 Rocket Propulsion

Average Burn Rate (Uniform Port)

- Continuing, $r(x) = \frac{dI_r}{dx} = aG_{ox} \left[1 + \frac{4\rho_s I_r}{D_P G_{ox}} \right]^n x^{-m}$
- Separate variables depending on x and on I_r , then integrate separately

$$I_r(x) = \frac{D_P G_{ox}}{4\rho_s} \left[\left(1 + \frac{4(1-n)a\rho_s x^{1-m}}{(1-m)D_P G_{ox}^{1-n}} \right)^{1/n} - 1 \right]$$

- Note:

$$r_{avg} = \frac{1}{x} \int_0^x r(x') dx' = \frac{I_r(x)}{x}$$

Hybrid Rockets 18
Copyright © 2007, 2017, 2019 by Jerry M. Seltman. All rights reserved.

AE6450 Rocket Propulsion

Average Burn Rate (Uniform Port)

- So average burn rate over distance x is

$$r_{avg} = \frac{D_p G_{ox}}{4\rho_s x} \left[\left(1 + \frac{4(1-n)a\rho_s x^{1-m}}{(1-m)D_p G_{ox}^{1-n}} \right)^{1/n} - 1 \right]$$

- Using Taylor expansion

$$r_{avg} \cong \left(\frac{a}{1-m} \right) G_{ox}^n x^{-m} \left(1 + \frac{2n \left(\frac{a}{1-m} \right) \rho_s x^{1-m}}{D_p G_{ox}^{1-n}} \right)$$

$$r_{avg} \cong a' G_{ox}^n x^{-m} \left(1 + 2na' \rho_s \frac{x^{1-m}}{D_p G_{ox}^{1-n}} \right) \sim a' G_{ox}^n x^{-m} (1 + \varepsilon)$$

*useful for prelim.
design process*

$$\dot{m}_f(t) = r_{avg}(L) \rho_s A_b \sim a' \rho_s S(t) G_{ox}^n(t) L^{1-m}$$

– get $S(t)$, $A_x(t)$ from regression rate

Example Regression Law Data

Polybutadiene/ LOx	Equation	All Motors			Small Motors			Large Motors
		n	m	Avg. Error	n	m	Avg. Error	Avg. Error
1	$aG^n L^m$	0.800	-0.200	5.5%	0.800	-0.200	3.9%	9.5%
2	$aG^n L^m$	0.763	-0.148	4.7%	0.829	-0.256	5.7%	13.9%
3	$aG_0^n L^m$	0.756	-0.165	6.4%	0.668	0.028	4.7%	38.5%
4	$aG_0^n L^m \left(1 + \frac{2an\rho L^{1+m}}{DG_0^{1+n}} \right)$	0.765	-0.162	5.1%	0.740	-0.103	4.9%	11.5%
5	$aG^n L^m \left(1 - \exp\left(\frac{-D}{1.06}\right) \right)$	0.767	-0.254	3.8%	0.757	-0.242	3.6%	3.5%
6	$aG_0^n L^m D^d \rho^{\phi_p}$	0.722	0.034	4.6%	0.633	0.076	4.3%	108.3%
		$\phi_p = -0.05$			$\phi_p = -0.046$			

*The large-motor errors are calculated using small-motor constants, indicating the scaling effects.

Table 7.5 Humble

Example Regression Law Data

Equation	All Motors			Small Motors			Large Motors
	n	m	Avg. Error	n	m	Avg. Error	Avg. Error
1 $aG_o^n L^m$	0.800	-0.200	19.0%	0.800	-0.200	15.2%	36.1%
2 $aG_o^n L^m$	0.676	-0.063	15.9%	0.749	-0.185	15.1%	27.9%
3 $aG_o^n L^m$	0.597	0.113	17.4%	0.618	0.142	17.8%	16.6%
4 $aG_o^n L^m \left(1 + \frac{2an\rho L(1+m)}{DG_o(1+n)}\right)$	0.645	0.025	18.8%	0.677	-0.016	19.0%	21.3%
5 $aG_o^n L^m \left(1 - e^{-\frac{D}{1.4}}\right) \left(1 - e^{-\frac{\rho}{625}}\right)$	0.535	-0.052	6.5%	0.547	-0.048	5.8%	10.1%
6 $aG_o^n L^m D^d \rho^{\phi_p}$	0.532	0.145	11.3%	0.565	0.027	6.7%	27.9%
	$\phi_p = 0.574$			$\phi_p = 0.677$			

*The large-motor errors are calculated using small-motor constants, indicating the scaling effects.

Table 7.6 Humble

Hybrid Rockets 2
Copyright © 2007, 2017, 2019 by Jerry M. Seltman. All rights reserved.

AE6450 Rocket Propulsion

Motor Ballistics

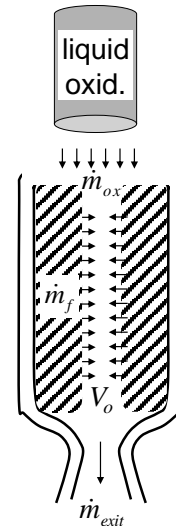
- As with solid motors, use mass conservation to determine motor conditions

$$0 = \frac{d}{dt}(\rho_o V_o) + \dot{m}_{exit} - (\dot{m}_f + \dot{m}_{ox})$$

$$\frac{V_o}{RT_o} \frac{dp_o}{dt} + \rho_o A_b r = (\rho_{sf} A_b r + \dot{m}_{ox}) - \dot{m}_{exit}$$

$$\frac{V_o}{RT_o} \frac{dp_o}{dt} = (\rho_{sf} - \rho_o) A_b r + \dot{m}_{ox}$$

$$-\frac{p_o}{\sqrt{RT_o}} \sqrt{\gamma} \left(\frac{2}{\gamma+1}\right)^{\frac{\gamma+1}{2(\gamma-1)}} A_t$$



Hybrid Rockets 22
Copyright © 2007, 2017, 2019 by Jerry M. Seltman. All rights reserved.

AE6450 Rocket Propulsion

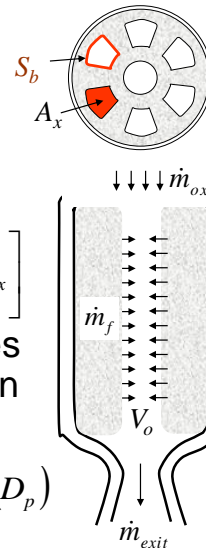
Motor Ballistics

- Using our model for the avg. regression rate $r_{avg} \cong a' G_{ox}^n L^{-m}$
 - and assuming quasi-steady operation with a high density fuel

$$p_o = \frac{\sqrt{RT_o/\gamma}}{A_t} \left(\frac{\gamma+1}{2} \right)^{\gamma+1/2(\gamma-1)} \left[a' \rho_{sf} L^{1-m} \frac{S_b}{A_x^n} \dot{m}_{ox}^n + \dot{m}_{ox} \right]$$

- possible time-dependent variables (nozzle erosion significant issue in oxidizer rich cases)

$$p_o = p_o(T_o, MW, \gamma, A_t, D_p, \dot{m}_{ox}) \quad S_p, A_x = f(D_p)$$



“Unsteady” Behavior

$$p_o = p_o(T_o, MW, \gamma, A_t, D_p, \dot{m}_{ox})$$

- Already know D_p changes with time
 - suggest p_o and therefore thrust may change with time
- From previous analysis, also know

$$\dot{m}_f(t) \propto S(t) G_{ox}^n(t) L^{1-m} = S(t) \left[\frac{\dot{m}_{ox}(t)}{A_x(t)} \right]^n$$

$$\frac{\dot{m}_{ox}}{\dot{m}_f} \propto \frac{[A_x(t)]^n}{S(t)} [\dot{m}_{ox}(t)]^{1-n}$$

- O/F ratio can also change with time

O/F Ratio

- Change in O/F with time $\frac{\dot{m}_{ox}}{\dot{m}_f} \propto \frac{[A_x(t)]^n}{S(t)} [\dot{m}_{ox}(t)]^{1-n}$
 - e.g., circular port $O/F \propto \dot{m}_{ox}^{1-n} D_P^{2n-1}$
 - for fixed oxid. flow rate $\frac{(O/F)_{final}}{(O/F)_{initial}} = \left(\frac{D_{P,final}}{D_{P,initial}} \right)^{2n-1}$
 $O/F \uparrow$ if $n > 0.5$
 - reduced "burn" rate even as A_b increase, because lower heat xfer
- estimate amount from volum. loading effc.

\equiv Volume Grain/Volume Chamber, typically ~ 0.6

$$\frac{D_{P,final}}{D_{P,initial}} \sim \frac{D_{chamber}}{D_{P,initial}} \sim \frac{(V_{chamber}/L)^{0.5}}{([V_{chamber} - V_{grain}]/L)^{0.5}} \sim \sqrt{\frac{1}{1 - V_{grain}/V_{chamber}}}$$

$$\frac{D_{P,final}}{D_{P,initial}} \sim \sqrt{\frac{1}{1 - 0.6}} \sim 1.6 \text{ for HTPB/LOX } n \sim 0.75 \quad \frac{(O/F)_{final}}{(O/F)_{initial}} \sim 1.3$$

O/F Ratio Importance

- Besides reduction in fuel mass flux through rocket, does change in O/F ratio have any other effects

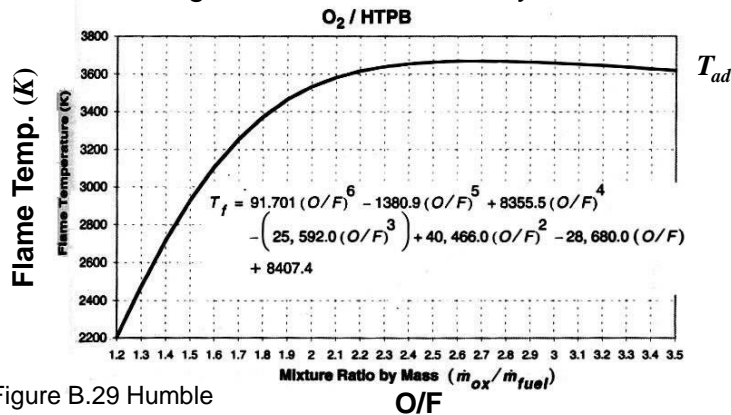


Figure B.29 Humble

O/F Ratio Importance

- Besides reduction in fuel mass flux through rocket, does change in O/F ratio have any other effects

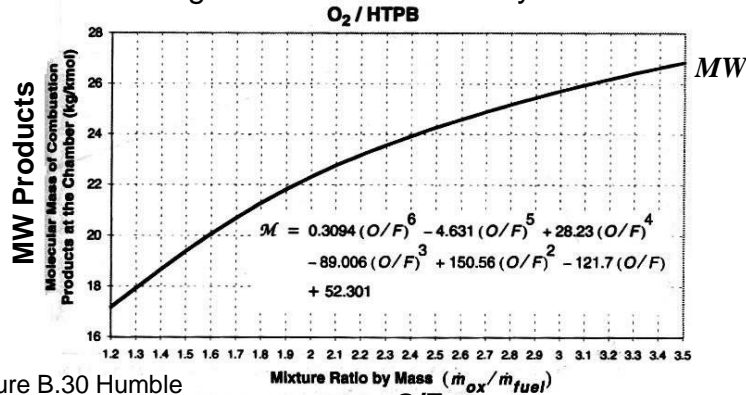


Figure B.30 Humble

$$p_o = p_o(T_o, MW) \quad c^* = c^*(T_o, MW) \Rightarrow p_o, c^* \text{ and thus } \tau I_{sp} \text{ unsteadiness}$$

Hybrid Rockets 27
Copyright © 2007, 2017, 2019 by Jerry M. Seltman. All rights reserved.

AE6450 Rocket Propulsion

O/F Ratio

- Again for circular port $O/F \propto \dot{m}_{ox}^{1-n} D_p^{2n-1}$
 - $n=0.5$ removes dependence on port size
 - freestream mass flux dependence of burn rate ($A_x^{0.5} \sim D$) cancels $\sim A_b (P \times L \sim D)$ dependence
 - but also likely results in lower regression rate

$$r_{avg} \sim d' G_{ox}^n x^{-m}$$

Hybrid Rockets 28
Copyright © 2007, 2017, 2019 by Jerry M. Seltman. All rights reserved.

AE6450 Rocket Propulsion

Oxidizer Control

- Can use oxidizer flow rate to control O/F

$$\frac{\dot{m}_{ox}}{\dot{m}_f} \propto \frac{[A_x(t)]^n}{S(t)} [\dot{m}_{ox}(t)]^{1-n}$$

- If O/F increasing then can offset by reducing oxidizer flow rate
 - but that means lower total mass flow rate through rocket
 - will tend to lower thrust, partly made up by increase in specific impulse, exit velocity
- If trying to throttle engine, same concerns

Throttling via Oxidizer Flowrate

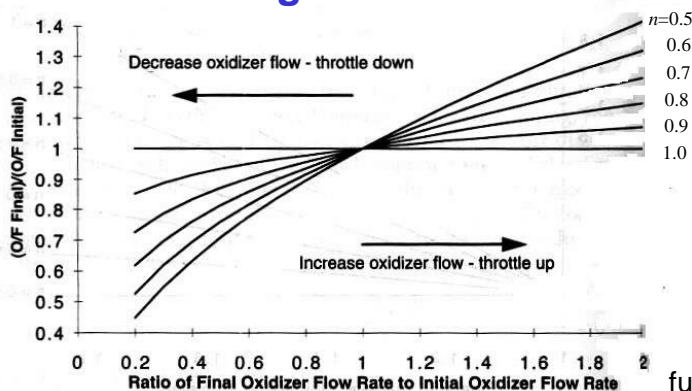


Figure 7.10
Humble

- weak dependence of O/F on G_{ox} for $n \rightarrow 1$ (G_f linearly proportional to G_{ox} in that case)
- when throttling down, usually $O/F \downarrow$ (richer), can add oxid. downstream of fuel to maintain constant O/F

